Role of potential structure in nonadiabatic collisions

Manoj Mishra,* Robert Guzman, and Herschel Rabitz
Department of Chemistry, Princeton University, Princeton, New Jersey 08540
(Received 11 March 1987)

The role of structure in crossing potential-energy curves upon nonadiabatic collisions is probed by means of functional sensitivity analysis. The inelastic transition $^2\Sigma[He^+ + Ne(3p^6)] \rightarrow {}^2\Sigma[He^+ + Ne(3p^5 4s)]$ modeled by a crossing of the corresponding diabatic potential-energy curves (V_{11} and V_{22}) is used as an illustration. The functional derivatives $\delta\sigma_{12}(E)/\delta V_{11}(R)$, $\delta\sigma_{12}(E)/\delta V_{22}(R)$, and $\delta\sigma_{12}(E)/\delta V_{12}(R)$ of the corresponding nonadiabatic collision cross section σ_{12} are calculated using the exponential distorted-wave approximation. These functional derivatives offer a quantitative measure of the importance of different regions of the potential [$V_{11}(R)$ and $V_{22}(R)$] and coupling [$V_{12}(R)$] functions to the nonadiabatic collision cross section σ_{12}. The prominent Gaussian-like feature of the $\delta\sigma_{12}(E)/\delta V_{12}(R)$ curve in the crossing point region ($R \sim R^*$) is found to be in qualitative accord with the $\delta(R - R^*)$ function idealization of the Landau-Zener-Stueckelberg (LZS) theory. Similarly, the most prominent feature of the $\delta\sigma_{12}(E)/\delta V_{11}(R)$ and $\delta\sigma_{12}(E)/\delta V_{22}(R)$ curves occurs in the vicinity of the crossing point region where they mimic the $d\delta(R - R^*)/dR$ behavior predicted by the LZS theory. The breadths of all three functional derivative curves identify a much broader region of potential function importance than the loosely defined avoided-crossing region. The region of significance is also found to increase with an increase in the total energy. This considerable sensitivity away from the crossing point along with the quantum interference structure of the functional sensitivity curves and the dynamical dependence of these sensitivities offer new insights and bring out the limitations of the intuitive pictures rooted in the LZS theory of curve crossing.

I. INTRODUCTION

An analysis of the role played by structure in a scattering potential V upon a cross section σ may be examined by a functional expansion:[1]

$$\sigma[V+\delta V]=\sigma[V]+\int dR' \frac{\delta\sigma}{\delta V(R')}\delta V(R') + O(\delta V)^2 + \cdots . \quad (1)$$

Here R' denotes generic coordinate space variables. For infinitesimal variations, we may limit ourselves to first order in the variation δV, whereby

$$\delta\sigma = \int dR' \delta V(R') \frac{\delta\sigma}{\delta V(R')} . \quad (2)$$

The first-order functional derivative $\delta\sigma/\delta V(R')$ serves the role of a weight function in Eq. (2) projecting out those regions of the potential of significance to the cross section. The values of R' for which $\delta\sigma/\delta V(R')$ is large imply regions of importance in the potential, while for R' values where $\delta\sigma/\delta V(R')$ is small, the sensitivity of the cross section will be negligible. An important point to note is that this assessment does not require an explicit variation $\delta V(R')$ but rather just an examination of the functional sensitivity $\delta\sigma/\delta V(R')$. A formal development of this technique may be found in earlier work[2,3] and this paper focuses on an application to nonadiabatic collisions.

The treatment of nonadiabatic collisions requires obtaining more than one potential energy curve (surface) and the corresponding nonadiabatic coupling elements.[4,5] The concept of curve crossings is central to most schemes attempting to explain electronic energy transfer in molecular collisions.[6] A study of the contributions made by different regions of these curves and the coupling matrix elements on nonadiabatic collision cross sections is of clear physical importance. Such a study could also isolate regions where the potential-energy curves and coupling elements need to be calculated accurately and others where a less accurate determination would suffice for a particular system.

The Landau-Zener-Stueckelberg[7] (LZS) theory of curve crossings has been utilized fruitfully in this context and its limitations have been explored by various workers.[6,8] The principal feature of this theory is the complete determination of the transition probability by the slope of the curves and the magnitude of the coupling between the states, at the point of the crossing *alone*. The corollary to this hypothesis is the irrelevance of further information on these curves and the coupling matrix element away from the crossing point. Insights about the validity of the assumptions of the Landau-Zener-Stueckelberg theory will be obtained as an adjunct of our analysis.

In Sec. II, we outline the formal apparatus for studying two state curve-crossing functional sensitivities. The inelastic transition $^2\Sigma[He^+ + Ne(3p^6)] \rightarrow {}^2\Sigma[He^+ + Ne(3p^5 4s)]$ has been modeled by the crossing of corresponding diabatic curves[9,10] and will be used as a simple application in Sec. III.

II. THEORY

The assumption of only two electronic states along with a partial-wave expansion of the scattering functions for both states leads to the following coupled radial equations

for the lth partial wave[10,11]

$$\left[\frac{d^2}{dR^2}+k_1^2-U_{11}(R)-\frac{l(l-1)}{R^2}\right]\chi_1^l(R) = U_{12}(R)\chi_2^l(R)\ , \tag{3a}$$

$$\left[\frac{d^2}{dR^2}+k_2^2-U_{22}(R)-\frac{l(l-1)}{R^2}\right]\chi_2^l(R) = U_{21}(R)\chi_1^l(R)\ , \tag{3b}$$

where

$$U_{21}=U_{12}=\frac{2\mu}{\hbar^2}V_{12}\ ,$$

$$k_i^2=\frac{2\mu}{\hbar^2}[E-V_{ii}(\infty)],\quad i=1,2$$

and $V_{12}(R)$ is the usual diabatic matrix element between the electronic wave functions for the two states.[11] In Eq. (3), μ is the collisional reduced mass, R is the internuclear distance, and the radial scattering wave functions for the electronic states 1 and 2 are $\chi_1^l(R)$ and $\chi_2^l(R)$, respectively.

The numerical solution of the coupled Eqs. (3) with the boundary condition $R\to\infty$

$$\chi_j^{li}(R)\sim k_i^{-1/2}\left\{\delta_{ij}\exp\left[-i\left[k_jR-\frac{l\pi}{2}\right]\right]-S_{ij}^l\exp\left[i\left[k_jR-\frac{l\pi}{2}\right]\right]\right\} \tag{4}$$

furnishes the elements of the scattering matrix $\underline{S}^l$, and the integral scattering cross section σ_{ij} is given by

$$\sigma_{ij}=\frac{\pi}{k_i^2}\sum_{l=0}^{\infty}(2l+1)\,|\,\delta_{ij}-S_{ij}^l\,|^2\ . \tag{5}$$

At the energies involved here ($\sim$25–75 eV) a viable approximation is computationally convenient. The exponential distorted-wave (EDW) approximation has been found to be very useful in this context[3(a),12] and is the method we have chosen for the present investigation. However, the general functional sensitivity approach is not limited to any particular dynamical approximation.

In the EDW approximation, the S matrix at a fixed angular momentum is given by

$$\underline{S}^l=\exp(i\underline{\eta}^l)\exp(-i\underline{B}^l)\exp(i\underline{\eta}^l)\ , \tag{6}$$

where $\underline{\eta}^l$ a diagonal matrix of phase shifts and the nonzero elements of the distorted-wave matrix $\underline{B}^l$ are given by

$$B_{21}^l=B_{12}^l=\frac{4\mu}{\hbar^2}[k_1k_2]^{1/2}\int_0^{\infty}dR w_l(k_1R)V_{12}(R)w_l(k_2R) \tag{7}$$

and $w_l(k_iR)$ is a distorted-wave (DW) function obtained by solving Eq. (3) without the off-diagonal coupling element.

The effect of variations in $V_{11}(R), V_{22}(R)$, or $V_{12}(R)$ on σ_{12} may now be ascertained by calculating $\delta\sigma_{12}/\delta V_{11}(R), \delta\sigma_{12}/\delta V_{22}(R)$, and $\delta\sigma_{12}/\delta V_{12}(R)$, respectively. The functional derivative $\delta\sigma_{12}/\delta V_{ij}(R)$ is given by

$$\frac{\delta\sigma_{12}}{\delta V_{ij}(R)}=\frac{2\pi}{k_1^2}\sum_l(2l+1)\mathrm{Re}\times\left[\exp[i\underline{B}^l]_{12}\frac{\delta\exp[-i\underline{B}^l]_{12}}{\delta V_{ij}(R)}\right]\ . \tag{8}$$

This may be simplified by drawing upon[13]

$$\frac{\delta\exp[-i\underline{B}^l]_{12}}{\delta V_{ij}(R)}=[\underline{Q}\underline{X}^{V_{ij}(R)}\underline{Q}^{-1}]_{12}\ , \tag{9}$$

where $\underline{Q}$ is the unitary transformation matrix that diagonalizes $\underline{B}^l$,

$$\underline{Q}^{-1}\underline{B}^l\underline{Q}=\underline{d}\ , \tag{10}$$

$$X_{mn}^{V_{ij}(R)}=P_{mn}^{V_{ij}(R)}Z_{mn}\ , \tag{11}$$

$$P_{mn}^{V_{ij}(R)}=\left[\underline{Q}^{-1}\left[\frac{\delta\underline{B}^l}{\delta V_{ij}(R)}\right]\underline{Q}\right]_{mn}\ , \tag{12}$$

and

$$Z_{mn}=\frac{\exp(-id_{mm})-\exp(-id_{nn})}{d_{mm}-d_{nn}}\ . \tag{13}$$

The partial-wave index l is implicitly understood to label all the matrices defined above.

Thus, in evaluating the functional sensitivities $\delta\sigma_{12}/\delta V_{ij}(R)$ we need to evaluate the corresponding derivatives $\delta B_{12}^l/\delta V_{ij}(R)$. To obtain these derivatives, we directly differentiate the expression in Eq. (7),

$$\frac{\delta B_{12}^l}{\delta V_{12}(R)}=\frac{4\mu}{\hbar^2}(k_1k_2)^{1/2}\int_0^{\infty}dR' w_l(k_1R')\frac{\delta V_{12}(R')}{\delta V_{12}(R)}w_l(k_2R') \tag{14a}$$

$$=\frac{4\mu}{\hbar^2}(k_1k_2)^{1/2}w_l(k_1R)w_l(k_2R)\ , \tag{14b}$$

$$\frac{\delta B_{12}^l}{\delta V_{11}(R)}=\frac{4\mu}{\hbar^2}(k_1k_2)^{1/2}\int_0^{\infty}dR'\frac{\delta w_l(k_1R')}{\delta V_{11}(R)}V_{12}(R')w_l(k_2R')\ , \tag{15}$$

and

$$\frac{\delta B_{12}^l}{\delta V_{22}(R)}=\frac{4\mu}{\hbar^2}(k_1k_2)^{1/2}\int_0^{\infty}dR' w_l(k_1R')V_{12}(R')\frac{\delta w_l(k_2R')}{\delta V_{22}(R')}\ . \tag{16}$$

The functional derivatives of the wave functions $\delta w_l(k_i R')/\delta V_{ii}(R)$ are obtained by solving their governing equation

$$\left[\frac{d^2}{dR'^2}-\frac{l(l+1)}{R'^2}+k_i^2-U_{ii}(R')\right]\frac{\delta w_l(k_i R')}{\delta V_{ii}(R)}=\frac{2\mu}{\hbar^2}\delta(R-R')w_l(k_i R') \ . \tag{17}$$

Using a Green's function approach[3(a)] to solving this equation combined with Eqs. (15) and (16) yields

$$\frac{\delta B_{12}^l}{\delta V_{ii}(R)}=\frac{4\mu}{\hbar^2}(k_1k_2)^{1/2}\left[\frac{w_l^\dagger(k_i R)w_l(k_i R)}{k_i}\int_0^R w_l(k_i R')U_{12}(R')w_l(k_j R')dR'\right.$$
$$\left.+\frac{w_l^\dagger(k_i R)}{k_i}\int_R^\infty w_l^\dagger(k_i R')U_{12}(R')w_l(k_j R')dR'\right], \quad i,j=1,2;i\neq j \tag{18}$$

where $w_l^\dagger$ is the irregular distorted wave function. The functional sensitivities $\delta\sigma_{12}/\delta V_{11}(R)$ and $\delta\sigma_{12}/\delta V_{22}(R)$ may now be obtained by using Eqs. (18) and (9) in Eq. (8). The expression for the functional sensitivity $\delta\sigma_{12}/\delta V_{12}(R)$ is obtained by using Eq. (14b) in conjunction with Eqs. (9) and (8). The evaluation of these quantities in the present calculations is facilitated by using Langer's uniform asymptotic expansion[14,15] for the radial wave function $w_l(k_i R)$ and $w_l^\dagger(k_i R)$.

III. RESULTS AND DISCUSSION

We have applied the method outlined in the previous section to examine the role of the potentials for the curve-crossing transition $^2\Sigma[He^+ + Ne(3p^6)]\rightarrow{}^2\Sigma[He^+ + Ne(3p^5 4s)]$ modeled by Smith and Olson.[10(a)] The diabatic curves are shown in Fig. 1 and are parametrized by the functional forms

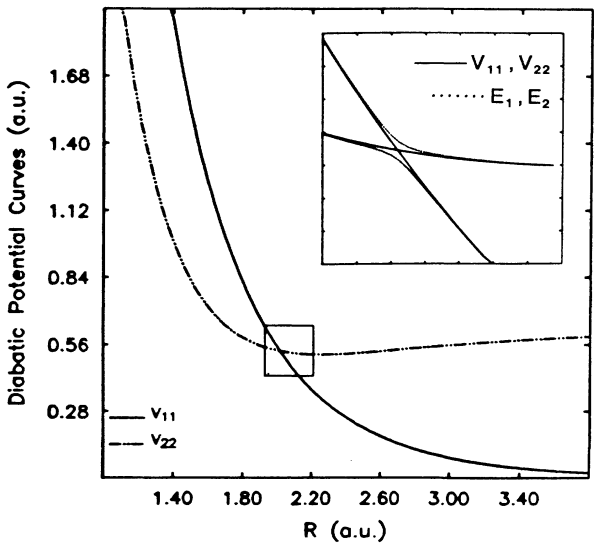

FIG. 1. The diabatic potentials $V_{11}(R)$ and $V_{22}(R)$ for $He^+ + Ne$ of Ref. 10(a), from which the present calculations were made. The corresponding adiabatic curves $E_1(R)$ and $E_2(R)$ are displayed in the inset. The domain of the inset corresponds to the boxed area of the main figure. Potential and crossing parameters are collected in Table I.

$$V_{11}(R)=a_1R^{-1}\exp(-R/a_2) \ , \tag{19}$$

$$V_{22}(R)=(a_1R^{-1}-a_3)\exp(-R/a_2)+16.8 \text{ eV} \ , \tag{20}$$

and

$$V_{12}(R)=a_4\exp(-R/a_5) \ . \tag{21}$$

The various parameters are those of Ref. 10(a) and are reproduced in Table I for convenience. The EDW calculations for the cross sections agree well with the DW [Ref. 10(a)] and the uniform WKB (UWKB) results[10(b)] as shown in Table II. Results for functional sensitivities for $E=0.919$ and 2.606 a.u. are presented in Figs. 2 and 3, respectively. In viewing these curves, both their magnitude and sign are physically significant. A large magnitude implies a significant region of the potential and the $+$ $(-)$ sign indicates whether an increase in the potential in that region will produce a concomitant increase (decrease) in the cross section.

All the sensitivities rapidly damp to zero in the nonclassical short-range region and display oscillatory structure for large internuclear distances with de Broglie wavelengths of π/k_1, π/k_2 and $2\pi/(k_1-k_2)$ for $\delta\sigma_{12}/\delta V_{11}(R)$, $\delta\sigma_{12}/\delta V_{22}(R)$, and $\delta\sigma_{12}/\delta V_{12}(R)$, respectively. The short-range lack of potential sensitivity is physically reasonable and its origin in Eq. (14) and (18) is quite evident through the behavior of $w_l(k_i R)$ for $R\rightarrow 0$ and reflects the vanishingly small probability of finding the projectile in the classically forbidden region. The most prominent feature of these sensitivities is that their maximum amplitude is in the vicinity of the crossing point ($R^*=2.02$ a.u.) where $\delta\sigma_{12}/\delta V_{12}(R)$ displays a Gaussian-like feature, and both $\delta\sigma_{12}/\delta V_{11}(R)$ and $\delta\sigma_{12}/\delta V_{22}(R)$ change sign in going from $R<R^*$ to $R>R^*$. It is also seen that the sign reversal of the latter

TABLE I. $He^+ + Ne$ potential parameters from Ref. 10(a). All values are in atomic units.

a_1	21.1
a_2	0.678
a_3	12.1
a_4	0.170
a_5	0.667

TABLE II. Total inelastic cross sections. All values are in atomic units.

Energy	This calculation	DW [Ref. 10(a)]	UWKB [Ref. 10(b)]
0.919	0.820	0.874	
1.0	0.842		0.873
1.5	0.818		0.844
2.0	0.765		0.779
2.6	0.709		0.719
2.606	0.706	0.729	

two curves are the opposite of each other.

To *understand* these features, we replace the exponential approximation for $\underline{S}^l$ in Eq. (8) by its lowest-order DW expansion in view of the small magnitude of B^l_{12} (found numerically to be much less than unity). With this approximation

$$\frac{\delta\sigma_{12}}{\delta V_{ij}(R)} \simeq \frac{2\pi}{k_1^2}\sum_l (2l+1)B^l_{12}\frac{\delta B^l_{12}}{\delta V_{ij}(R)} \tag{22}$$

and using Eqs. (14) and (18) we obtain

$$\frac{\delta\sigma_{12}}{\delta V_{ij}(R)} \simeq \frac{8\pi\mu}{\hbar^2}\left[\frac{k_2}{k_1^3}\right]^{1/2}\sum_l (2l+1)B^l_{12}w_l(k_1R)w_l(k_2R) \tag{23}$$

and

$$\frac{\delta\sigma_{12}}{\delta V_{ii}(R)} \simeq -\frac{8\pi\mu}{\hbar^2}\left[\frac{k_2}{k_1^3}\right]^{1/2}\sum_l (2l+1)B^l_{12}\left[\frac{w_l^\dagger(k_iR)w_l(k_iR)}{k_i}\int_0^R w_l(k_iR')U_{12}(R')w_l(k_jR')dR' + \frac{w_l^2(k_iR)}{k_i}\int_R^\infty w_l^\dagger(k_iR')U_{12}(R')w_l(k_jR')dR'\right], \quad i,j=1,2;i\neq j\ . \tag{24}$$

Before we begin our analysis of Eqs. (23) and (24) to understand the sensitivity maps of Figs. 2–4 we note the following features of the diabatic curves of Fig. 1. For $R<R^*$ (the crossing point is R^*) we have $V_{11}(R)>V_{22}(R)$ while the reverse is true for $R>R^*$. As we increase l, the turning points for the corresponding effective potentials $[U_{jj}(R)+(l+1/2)^2/R^2]$ will keep moving to the right. These observations imply that while for lower values of l the turning point for $V_{11}(R)$ will occur for a larger R value than that for $V_{22}(R)$ as we increase l, the two turning points will begin to come closer to each other with minimum distance between the two at a value l^* that places the two turning points at or extremely close to the crossing point itself. As we go to l values higher than l^*, the two turning points will begin to diverge from each other and the crossing point. For sufficiently large l, the two turning points will be so far from the crossing point that the probability for transition from one curve to another will be vanishingly small leading to the truncation of the series in Eq. (5). In order to facilitate the discussion below we recall that the regular wave function $w_l(k_iR)$ starts out with vanishing amplitude in the nonclassical region and achieves its maximum amplitude immediately to the right of the turning point. The irregular wave function $w_l^\dagger(k_iR)$ on the other hand, goes to infinity in the nonclassical region. For large R values, the regular and irregular wave functions behave as $\sin(k_iR-l\pi/2+\eta_l)$ and $\cos(k_iR-l\pi/2+\eta_l)$, respectively.

The prominent Gaussian-like feature of $\delta\sigma_{12}(E)/\delta V_{12}(R)$ in Figs. 2–4 is now easily understood. At each l, the R dependence of Eq. (23) comes from the product of the regular wave functions $w_l(k_1R)$ and $w_l(k_2R)$. The maximum amplitude of these functions is very close to the turning point. For $l=l^*$, the turning points of both $V_{11}(R)$ and $V_{22}(R)$ will be at or very close to $R\simeq R^*$, and both $w_l(k_1R)$ and $w_l(k_2R)$ will be in phase with each other with their maxima nearly coinciding at $R\simeq R^*$. This explains the Gaussian-like feature of $\delta\sigma_{12}(E)/\delta V_{12}(R)$ with its maximum at $R\simeq R^*$. The width of this Gaussian-like feature at a particular total energy E will be determined by how rapidly the two wave functions go out of phase as a function of R. As we increase E, the two wave functions will become more and more coherent and will remain in phase over a larger range of R values thereby leading to an increase in the width of the Gaussian-like feature centered at $R\simeq R^*$. Also, since B_{12} decreases with an increase in E, the amplitude of $\delta\sigma_{12}(E)/\delta V_{12}(R)$ will tend to be smaller with an increase in E. Furthermore, since the outermost turning point shifts to lower R values with an increase in E, $\delta\sigma_{12}(E)/\delta V_{12}(R)$ will be nonzero for smaller R values as we increase E. All these features are seen in Figs. 2–4.

As we go to larger R values, we may replace $w_l(k_1R)$ and $w_l(k_2R)$ by their asymptotic forms in Eq. (23) leading to

$$\frac{\delta\sigma_{12}(E)}{\delta V_{ii}(R)} \sim \frac{-8\pi\mu}{\hbar^2}\left[\frac{k_2}{k_1^3}\right]^{1/2}\left\{\cos[(k_1-k_2)R]\sum_l (2l+1)B^l_{12}\left[\sin^2\left[\frac{l\pi}{2}+\eta_l\right]-\tfrac{1}{2}\right] - \tfrac{1}{2}\sin[(k_1+k_2)R]\sum_l (2l+1)B^l_{12}\left[\sin\left[\frac{l\pi}{2}+\eta_l\right]-1\right]\right\}. \tag{25}$$

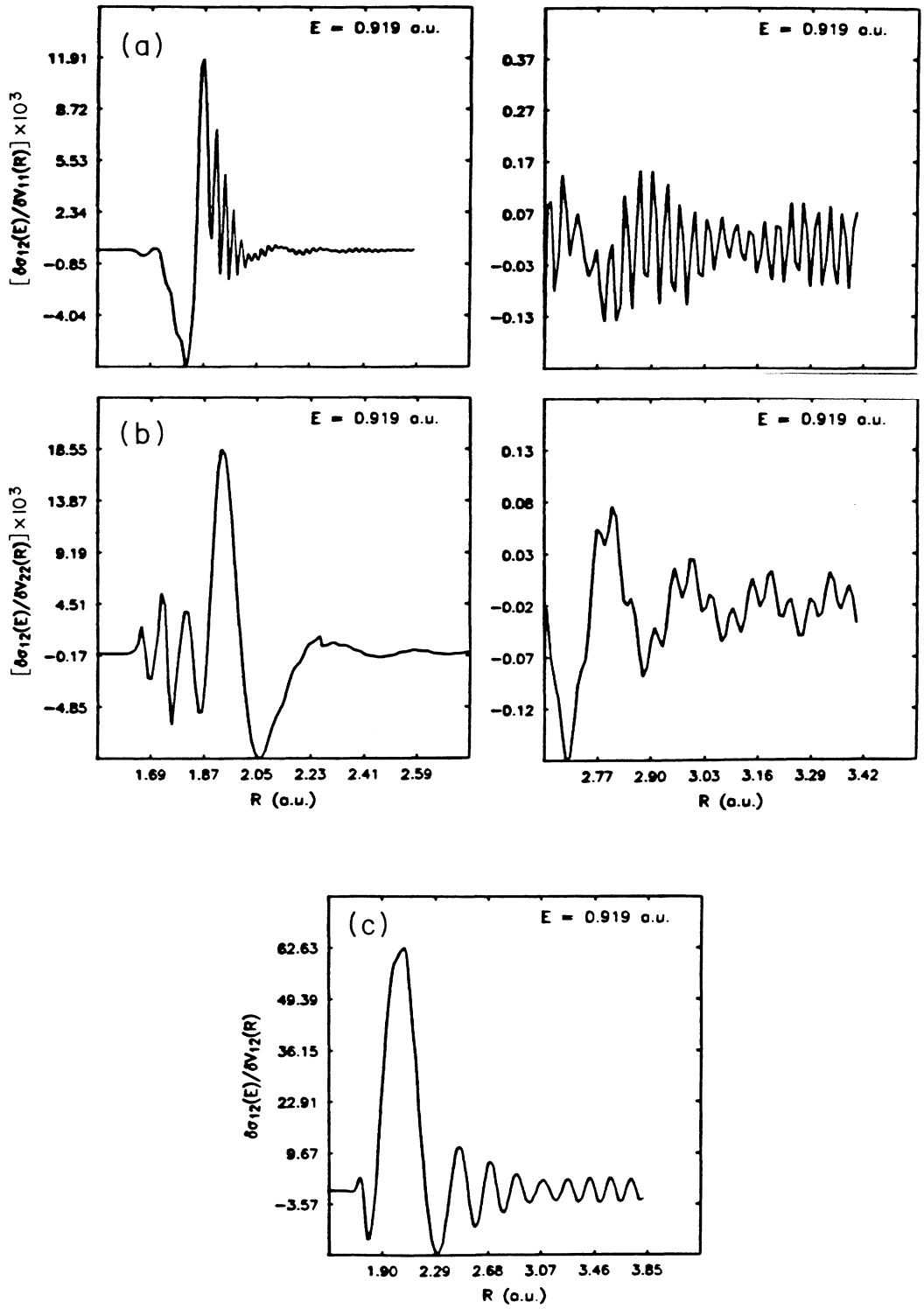

FIG. 2. Sensitivity profiles for (a) $\delta\sigma_{12}(E)/\delta V_{11}(R)$, (b) $\delta\sigma_{12}(E)/\delta V_{22}(R)$, and (c) $\delta\sigma_{12}(E)/\delta V_{12}(R)$ at $E=0.919$ a.u. as a function of the internuclear distance R. The maximum sensitivity for V_{12} and the derivative nature of the profile for V_{11} and V_{22} in the vicinity of the crossing point is in qualitative agreement with the predictions of the Landau-Zener-Stueckelberg theory. However, the width and the prominent features away from the crossing point expose its limitation. Details of the large-R behavior of $\delta\sigma_{12}(E)/\delta V_{11}(R)$ and $\delta\sigma_{12}(E)/\delta V_{22}(R)$ are amplified separately to the right. The large-R oscillatory structure of $\delta\sigma_{12}(E)/\delta V_{11}(R)$, $\delta\sigma_{12}(E)/\delta V_{22}(R)$, and $\delta\sigma_{12}(E)/\delta V_{12}(R)$ with wavelengths of π/k_1, π/k_2, and $2\pi/(k_1-k_2)$ are in agreement with asymptotic analysis.

In both Figs. 2(c) and 3(c) we observe a sinusoidal behavior with wavelength $2\pi/(k_1-k_2)$ with no evidence for the high-frequency term $2\pi/(k_1+k_2)$. The more coherent cosine terms apparently have a larger magnitude.

The large R behavior of $\delta\sigma_{12}(E)/\delta V_{ii}(R)$ is given by

$$\frac{\delta\sigma_{12}(E)}{\delta V_{ii}(R)} \sim \frac{-8\pi\mu}{\hbar^2}\left[\frac{k_2}{k_1^3}\right]^{1/2}\left[\sin(2k_1R)\sum_l (2l+1)(B^l_{12})^2\cos(2\eta^i_l - l\pi) + \cos(2k_1R)\sum_l (2l+1)(B^l_{12})^2\sin(2\eta^i_l - l\pi)\right], \quad i=1,2 \tag{26}$$

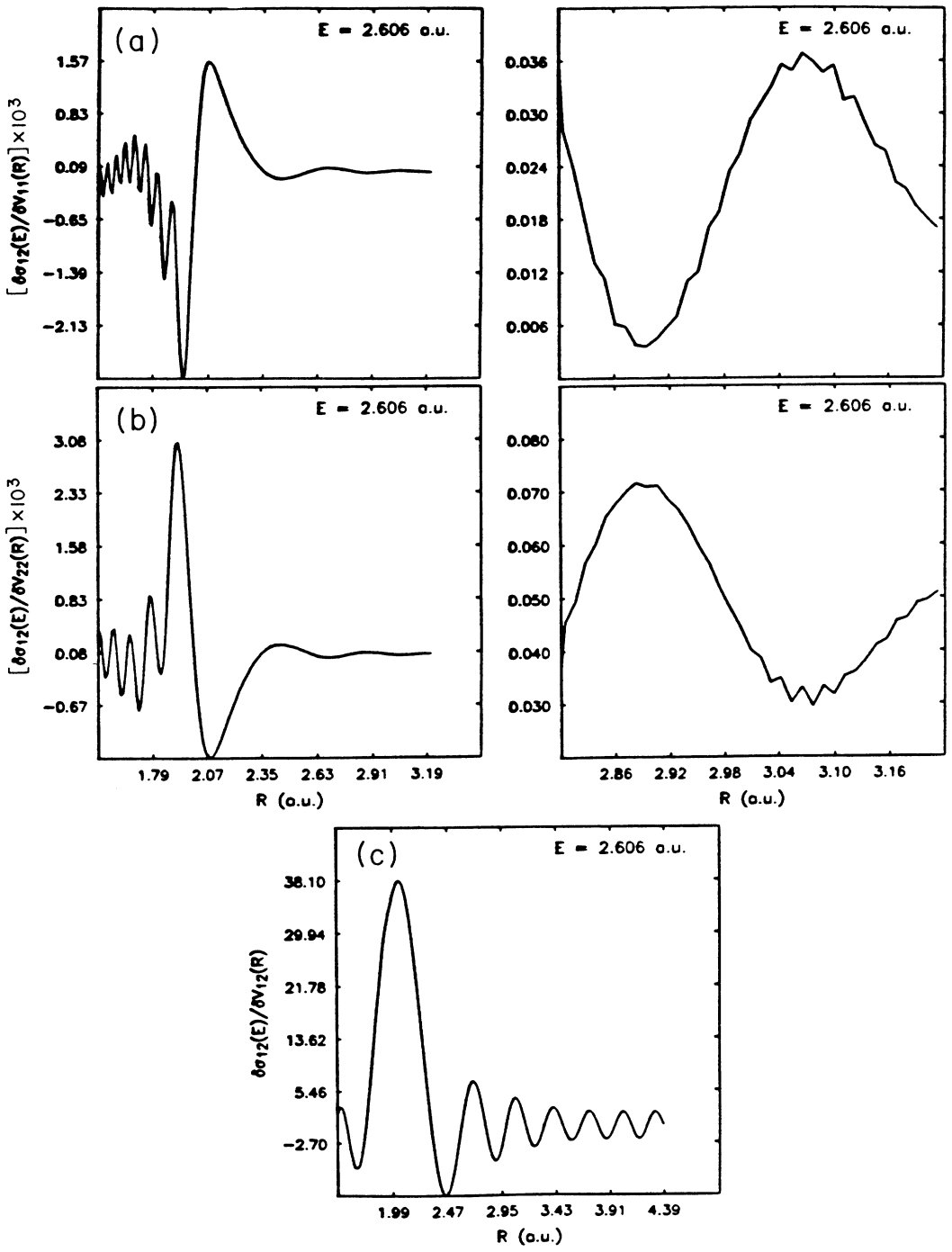

FIG. 3. Same as Fig. 2, except $E=2.606$ a.u.

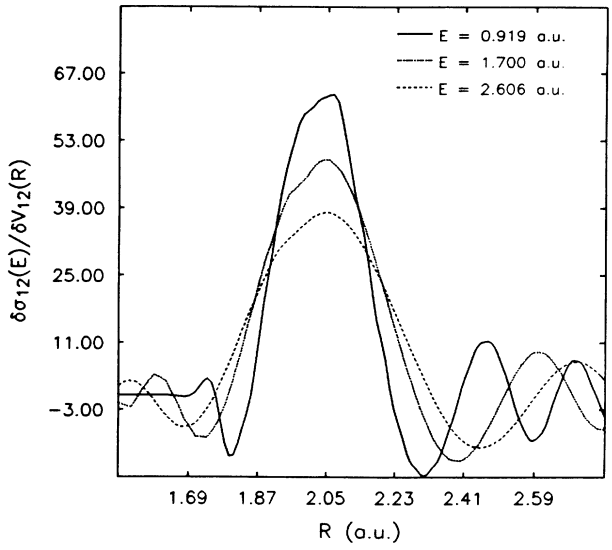

FIG. 4. Sensitivity profiles for $\delta\sigma_{12}(E)/\delta V_{12}(R)$ at different incident kinetic energies. The width of the Gaussian centered at the crossing point R^* is seen to be much larger than the avoided crossing region of Fig. 1 and its increase for higher E values underscores the limitation of intuitive pictures rooted in the LZS theory.

where we have used the asymptotic expansion for the wave functions. The sinusoidal behavior with wavelength $2\pi/k_i$ is seen in Figs. 2 and 3. The low-frequency modulating amplitude evident in these figures is not retained in the DW asymptotic form of Eq. (26). Recalling that the sensitivities act as a weight function in the integrand of Eq. (2) our findings imply that a broad variation $\delta V(R')$ in the asymptotic region would significantly affect σ_{12} if it had the proper high-frequency components (i.e., a simple Gaussian-like broad variation will elicit essentially a null response). This conclusion applies to the variations of V_{11}, V_{22}, and V_{12}.

From the behavior of the wave functions, it is evident that the major contribution to the dominant features of the R dependence of $\delta\sigma_{12}(E)/\delta V_{ii}(R)$ for a particular l value comes from the vicinity of the turning point for this l. Conversely, it may therefore be argued that the R dependence near the crossing point is controlled by a cluster of l values centered around l^* (since for $l=l^*$, both of the turning points are either at or very close to the crossing point). The leading contributions to the R dependence of $\delta\sigma_{12}(E)/\delta V_{ii}(R)$ in the vicinity of the crossing point is then provided by the second integral

$$w_l^2(k_iR)\int_R^\infty w_l^\dagger(k_iR')U_{12}(R')w_l(k_jR')dR' ,$$
$$i,j=1,2;i\neq j \qquad (27)$$

in Eq. (24) since the first integral will be over a small interval just about the turning point. Since $w_l^2(k_iR)$ is always positive, the sign of the leading R behavior is controlled by the integral $\int_R^\infty w_l^\dagger(k_iR')U_{12}(R')w_l(k_jR')dR'$. The leading R dependence of $\delta\sigma_{12}(E)/\delta V_{11}(R)$ and $\delta\sigma_{12}(E)/\delta V_{22}(R)$ may then be analyzed by examining the nature of this integral for $l<l^*$ and $l>l^*$.

For $l<l^*$, the turning point for $V_{22}(R)$ is to the left of the turning point for $V_{11}(R)$, with maximum positive amplitudes of $w_l^\dagger(k_1R)$ and $w_l(k_2R)$ in phase with each other. This leads to the integral $\int_R^\infty w_l^\dagger(k_1R')U_{12}(R')w_l(k_2R')dR'$ in Eq. (27) for $i=1$ being large and positive for $l<l^*$, i.e., $R<R^*$. In the same vein, when $l>l^*$ the maximum positive amplitude of $w_l^\dagger(k_1R)$ coincides with large negative portions of $w_l(k_2R)$ whereby the same integral is large but negative for $l>l^*$. Thus the positive leading behavior for $R<R^*$ changes into a negative leading behavior for $R>R^*$. Since the obverse of the logic employed for analyzing the behavior of $\int_R^\infty w_l^\dagger(k_1R')U_{12}(R')w_l(k_2R')dR'$ applies for $\int_R^\infty w_l^\dagger(k_2R')U_{12}(R')w_l(k_1R')dR'$, the positive and negative regions are reversed in this case, producing the opposite sign behavior of the main features of $\delta\sigma_{12}(E)/\delta V_{11}(R)$ and $\delta\sigma_{12}(E)/\delta V_{22}(R)$ as seen in Figs. 2 and 3.

Apart from the structures analyzed above, we also find that while the sensitivity maps of $\delta\sigma_{12}(E)/\delta V_{ij}(R)$ at different energies have similar gross features and identify approximately the same region of potential-energy curves as having a critical role in the collision process, the functional sensitivities also display a considerable energy dependence and a general decrease in magnitude with an increase in E. This is physically reasonable since at higher energy the projectile is less sensitive to structural features in the potential energy curves. Since the crossing point region is of central importance in the Landau-Zener-Stueckelberg theory of curve crossing, it is useful to examine functional sensitivities of σ_{12} in the framework of this theory. Towards this end, we substitute the LZS expression[7] for $|S_{12}^l|^2$ in Eq. (5)

$$|S_{12}^l|^2_{\rm LZS}=2\exp(-\xi/v_l)[1-\exp(-\xi/v_l)] , \qquad (28a)$$

where

$$\xi=\frac{2\pi}{\hbar}\frac{V_{12}^2(R^*)}{\left|\dfrac{dV_{11}}{dR}-\dfrac{dV_{22}}{dR}\right|_{R=R^*}} \qquad (28b)$$

and v_l is the radial velocity at R^* given by

$$\tfrac{1}{2}\mu v_l^2=E-V_{11}(R^*)-\frac{\hbar^2}{2\mu}\frac{l(l+1)}{R^{*2}} . \qquad (29)$$

Because of the factor $(2l+1)$, dominant contributions to Eq. (5) come from large values of l. Hence, following Bates and Lewis,[16] by replacing the summation in Eq. (5) by an integral, we can obtain the LZS functional sensitivities

$$\frac{\delta\sigma_{12}^{\rm LZS}}{\delta V_{12}(R)}=\frac{2V_{12}(R^*)}{\Delta\rho}\Omega\delta(R-R^*) , \qquad (30)$$

$$\frac{\delta\sigma_{12}^{\rm LZS}}{\delta V_{11}(R)}=\frac{V_{12}^2(R^*)}{(\Delta\rho)^2}\Omega\frac{d\delta(R-R^*)}{dR} , \qquad (31)$$

and

$$\frac{\delta\sigma_{12}^{\rm LZS}}{\delta V_{22}(R)}=-\frac{V_{12}^2(R^*)}{(\Delta\rho)^2}\Omega\frac{d\delta(R-R^*)}{dR} , \qquad (32)$$

where

$$\Delta\rho = \left| \frac{dV_{11}}{dR} - \frac{dV_{22}}{dR} \right|_{R=R^*} , \qquad (33)$$

$$\Omega = \frac{2\pi}{k_1^2}[2E_2(2\tau x) - E_2(\tau x)] ,$$

$$\tau = \frac{\pi\mu V_{12}^2(R^*)}{\hbar\Delta\rho[E - V_{11}(R^*)]} \qquad (34)$$

and $E_2(\tau x)$ is an exponential integral.[17]

From Figs. 2–4 it is apparent that the predictions of the Landau-Zener-Stueckelberg theory are in qualitative agreement with our results, with the obvious exception that the δ-function idealization is untenable. However, intutively one would expect from the assumptions of the LZS theory that the appropriate region of significance would be the loosely defined avoided-crossing region of the corresponding adiabatic curves (see the inset of Fig. 1). Even if allowance is made for the broader avoided-crossing region of the adiabatic curves (~0.1 a.u.), it falls short of the much broader region (~0.4 a.u.) of sensitivity centered at R^* seen in our results. The dynamical dependence of these sensitivities is also unaccounted for by the static intuitive picture rooted in the LZS theory.

In conclusion, we have presented a sensitivity method for establishing the significant regions of potential functions for two state nonadiabatic collision cross sections. The results obtained for $He^+ + Ne$ offer a useful example of the technique. The use of curve crossing to model nonadiabatic transitions is quite common [see Ref. 18 for a recent example] and the technique we have presented should be helpful in assessing the requisite level of accuracy needed for various regions of the potential energy curves and coupling matrix elements. While the importance of the broadly defined curve-crossing region is clearly brought out by our investigation, it is also obvious that the idealizations of the Landau-Zener-Stueckelberg theory have serious limitations.

The method we have outlined, includes only two electronic states but the generalization to include more electronic states is straightforward. Such a generalization is essential for treating intramultiplet transitions. The modeling of the inelastic $^2\Sigma[He^+ + Ne(3p^6)] \rightarrow {}^2\Sigma[He^+ + Ne(3p^5 4s)]$ transition by two repulsive diabatic curves, though effective and useful, perhaps masks other intriguing physical features of the functional sensitivity profiles $(\delta\sigma_{12}(E)/\delta V_{ij}(R))$ and regions of potential significance because of the simplicity of the curves themselves. Finally, a completely analogous theory may be developed within the framework of the close-coupling method or other desirable dynamic approaches.

ACKNOWLEDGMENT

We gratefully acknowledge the support for this work from the U.S. Department of Energy.

*Present address: Department of Chemistry, Indian Institute of Technology, Bombay 400 076, India.

[1]P. Hangii, *Stochastic Processes Applied to Physics,* edited by L. Pesquera and E. Santus (World Scientific, Singapore, 1985).

[2]R. Larter and H. Rabitz, Phys. Rev. A **29**, 1059 (1984).

[3](a) R. Guzman and H. Rabitz, Chem. Phys. **85**, 3277 (1986); (b) R. Judson and H. Rabitz, J. Chem. Phys. (to be published); (c) S. Shi and H. Rabitz, J. Chem. Phys. (to be published).

[4]For example, D. Secrest, in *Atom Molecule Collision Theory: A Guide for the Experimentalist,* edited by R. B. Bernstein (Plenum, New York, 1979).

[5]F. Rebentrost, in *Theoretical Chemistry: Advances and Perspectives,* edited by D. Henderson (Academic, New York, 1981); M. S. Child, in *Atom Molecular Collision Theory: A Guide for the Experimentalist,* edited by R. B. Bernstein (Plenum, New York, 1979); J. C. Tully, in *Dynamics of Molecular Collisions,* edited by W. H. Miller (Plenum, New York, 1976), Part. B.

[6]J. T. Yardley, *Introduction to Molecular Energy Transfer* (Academic, New York, 1980), pp. 205–227, and references therein; J. Simons, *Energetic Principles of Chemical Reactions* (Jones and Bartlett, Boston, 1983), p. 91; M. Baer, in *Theory of Chemical Reaction Dynamics,* edited by M. Baer (CRC Press, Boca Raton, 1985), pp. 260–263.

[7]L. Landau, Sov. Phys. **2**, 46 (1932); C. Zener, Proc. R. Soc. London, Ser. A **137**, 696 (1933); E. C. G. Stueckelberg, Helv. Phys. Acta. **5**, 369 (1932).

[8]D. R. Bates, Proc. R. Soc. London, Ser. A **257**, 22 (1960); E. E. Nikitin, *Chemische Elementarprozesse,* edited by H. Hartman (Springer-Verlag, Berlin, 1968), p. 43; M. S. Child, Mol. Phys. **20**, 171 (1971).

[9]D. Coffey, Jr., D. C. Lorents, and F. T. Smith, Phys. Rev. **87**, 201 (1969).

[10](a) R. E. Olson and F. T. Smith, Phys. Rev. A **3**, 1607 (1971); (b) B. C. Eu and T. P. Tsien, *ibid.* **7**, 648 (1973).

[11]F. T. Smith, Phys. Rev. **179**, 111 (1969); S. A. Evans, J. S. Cohen and N. F. Lane, Phys. Rev. A **4**, 2235 (1971).

[12]L. A. Eslava, L. Eno, and H. Rabitz, J. Chem. Phys. **73**, 4998 (1980).

[13]J. T. Hwang and H. Rabitz, J. Chem. Phys. **70**, 4609 (1979).

[14]M. S. Child, *Molecular Collision Theory* (Academic, New York, 1976).

[15]R. E. Langer, Phys. Rev. **51**, 669 (1937); W. D. Smith and R. T. Pack, J. Chem. Phys. **70**, 4609 (1979).

[16]D. R. Bates and J. T. Lewis, Proc. Phys. Soc. London, Sect. A **68**, 173 (1985).

[17]*Handbook of Mathematical Functions,* Natl. Bur. Stand. Appl. Math. Ser. No. 55, edited by M. Abramowitz and I. E. Stegun (U.S. GPO, Washington, D.C., 1972), p. 245.

[18]M. H. Alexander, in *Gas Phase Chemiluminiscence and Chemi-Ionization,* edited by A. Fontijn (Elsevier, New York, 1985), p. 221.